Universal fractal scaling in stream chemistry and its implications for solute transport and water quality trend detection

James W. Kirchner[a,b,c,1] and Colin Neal[d]

[a]Department of Environmental System Sciences, ETH Zürich, CH-8092 Zürich, Switzerland; [b]Swiss Federal Research Institute WSL, CH-8903 Birmensdorf, Switzerland; [c]Department of Earth and Planetary Science, University of California, Berkeley, CA 94720; and [d]Centre for Ecology and Hydrology, Wallingford OX10 8BB, United Kingdom

Edited by Andrea Rinaldo, Laboratory of Ecohydrology (IIE/ENAC), Ecole Polytechnique Federale, Lausanne, Switzerland, and approved June 6, 2013 (received for review March 8, 2013)

The chemical dynamics of lakes and streams affect their suitability as aquatic habitats and as water supplies for human needs. Because water quality is typically monitored only weekly or monthly, however, the higher-frequency dynamics of stream chemistry have remained largely invisible. To illuminate a wider spectrum of water quality dynamics, rainfall and streamflow were sampled in two headwater catchments at Plynlimon, Wales, at 7-h intervals for 1–2 y and weekly for over two decades, and were analyzed for 45 solutes spanning the periodic table from H^+ to U. Here we show that in streamflow, all 45 of these solutes, including nutrients, trace elements, and toxic metals, exhibit fractal $1/f^\alpha$ scaling on time scales from hours to decades ($\alpha = 1.05 \pm 0.15$, mean ± SD). We show that this fractal scaling can arise through dispersion of random chemical inputs distributed across a catchment. These $1/f$ time series are non–self-averaging: monthly, yearly, or decadal averages are approximately as variable, one from the next, as individual measurements taken hours or days apart, defying naive statistical expectations. (By contrast, stream discharge itself is nonfractal, and self-averaging on time scales of months and longer.) In the solute time series, statistically significant trends arise much more frequently, on all time scales, than one would expect from conventional *t* statistics. However, these same trends are poor predictors of future trends—much poorer than one would expect from their calculated uncertainties. Our results illustrate how $1/f$ time series pose fundamental challenges to trend analysis and change detection in environmental systems.

aquatic chemistry | watershed hydrology | environmental monitoring | pink noise | flicker noise

Trends in stream chemistry are widely used to monitor the environmental health of the surrounding landscape (1–3), and the chemical dynamics of aquatic environments can affect the health, genetics, diversity, and ecology of their organisms (4–7). Solute dynamics in streamwater also provide important clues to the structure and function of headwater drainage basins, which regulate the delivery of water, sediment, nutrients, and contaminants to rivers and lakes downstream (8, 9). Time series of chemically passive tracers, including Cl^-, ^{18}O, and ^2H, can be used to measure time scales of storage, mixing, and transport in drainage basins and stream networks (10, 11). Time series of chemically reactive solutes, on the other hand, can be used to infer runoff flow paths and quantify biogeochemical processes (12, 13).

Long-term trends in stream water quality have been documented for decades (1–3), and high-frequency dynamics have more recently been studied for individual solutes of interest (14–16), but until now, data limitations have hindered efforts to systematically survey the dynamics of stream chemistry across a wide range of solutes and time scales. For this purpose, the hydrochemical time series at Plynlimon, Wales, provide a data resource that is unique worldwide. Rainfall and streamflow in two headwater catchments, the Upper and Lower Hafren (*SI Appendix*, Fig. S1), have been sampled at 7-h intervals for 1–2 y (17, 18) and weekly for over two decades (19). Each of these samples has been analyzed for dozens of solutes, spanning six orders of magnitude in concentration and including every row of the periodic table (*SI Appendix*, Tables S1 and S2). The 45 analytes presented here include alkali metals (Li, Na, K, Rb, and Cs), alkaline earths (Be, Mg, Ca, Sr, and Ba), transition metals (Al, Sc, Ti, V, Cr, Mn, Fe, Co, Ni, Cu, Zn, Mo, Cd, Sn, and Pb), nonmetals (B, NO_3^-, NH_4^+, SO_4^{-2}, total S, Si, As, and Se), halogens (Cl^- and Br^-), and lanthanides and actinides (La, Ce, Pr, and U), as well as total dissolved nitrogen (TDN), dissolved organic nitrogen (DON), dissolved organic carbon (DOC), Gran alkalinity, pH, and electrical conductivity.

These water quality time series vary on all measurable time scales, from hours to decades (Fig. 1 and *SI Appendix*, Fig. S2), and thus are natural candidates for spectral analysis. Spectral analysis is widely used for detecting periodic signals, but is also particularly useful for evaluating persistence in time series (20). A spectral slope of zero indicates a time series with no persistence (white noise). Spectral slopes between zero and 1 indicate a stationary time series with weak persistence, whereas spectral slopes steeper than 1 imply nonstationarity and strong persistence (20). Time series with spectral slopes of 1, termed $1/f$ noises because their spectral power is inversely proportional to frequency, mark the threshold between stationarity and nonstationarity.

Results and Discussion

All 45 solutes in streamflow show clear fractal $1/f^\alpha$ power spectra, with power-law slopes close to $\alpha = 1$ (Figs. 2 and 3 and *SI Appendix*, Fig. S6). Many solutes exhibit seasonal cycles in streamwater (19) and their associated spectral peaks are clearly visible, but only in five cases (DOC, NO_3^-, K, Fe, and As) do they account for more than 30% of the variance in the long-term record. Likewise, many solutes exhibit diurnal cycles, particularly during low-flow recessions (17), but they never account for more than 3% of the variance in the high-frequency data sets.

Thus, the dominant feature of the streamflow concentration spectra is the clear inverse proportionality between spectral power and frequency, termed $1/f$ scaling. This fractal scaling cannot go on forever in either direction; each spectrum must be shallower than $1/f$ below some low-frequency limit (otherwise it implies a time

Author contributions: J.W.K. and C.N. designed research; J.W.K. developed new data analysis techniques; C.N. performed research; J.W.K. and C.N. analyzed data; and J.W.K. wrote the paper.

The authors declare no conflict of interest.

This article is a PNAS Direct Submission.

[1]To whom correspondence should be addressed. E-mail: kirchner@ethz.ch.

This article contains supporting information online at www.pnas.org/lookup/suppl/doi:10.1073/pnas.1304328110/-/DCSupplemental.

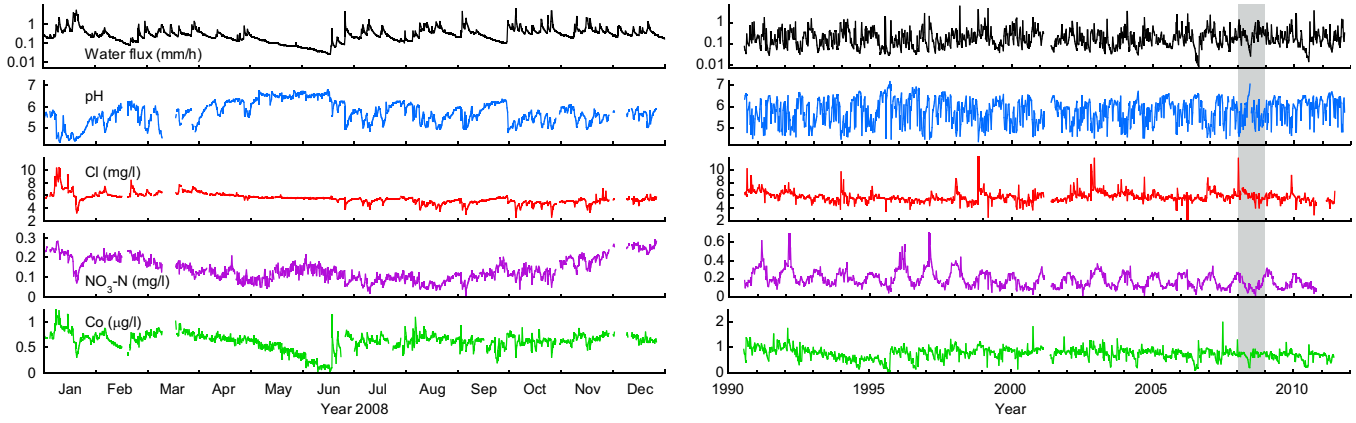

Fig. 1. Water quality time series in Upper Hafren streamwater, Plynlimon, Wales, at 7-h intervals for 1 y (*Left*) and weekly intervals for 21 y (*Right*). Four examples from the 45 water quality parameters are shown: pH (an indicator of acid–base status), chloride (a passive chemical tracer, derived mostly from sea salt deposition), nitrate (a nutrient that exhibits both diurnal and seasonal cycles), and cobalt (a trace metal which can function as both a micronutrient and a toxin). Shaded band (*Right*) shows the time interval covered on *Left*. Time series for all 45 solutes are shown in *SI Appendix*, Fig. S2.

series with infinite variance), and each spectrum must also be steeper than $1/f^2$ above some high-frequency limit (otherwise it implies that the underlying process is discontinuous). Nonetheless, most of the 45 solutes show clear $1/f$ scaling that spans 3–4 orders of magnitude, from hours to decades, the full range of time scales visible in the data.

The spectral slopes of all 45 solutes cluster in relatively narrow ranges: 1.03 ± 0.11 and 1.06 ± 0.15 (means ± SDs) in Upper and Lower Hafren streamwater, respectively (Fig. 3 and *SI Appendix*, Table S5). In bulk precipitation, these same solutes have much flatter power spectra, with slopes of 0.36 ± 0.09. There is a tendency for anions and other weakly sorbing solutes in streamwater to have steeper spectral slopes than the average (e.g., Cl^-, NO_3^-, SO_4^{-2}, and DOC, as well as conductivity and Na, which are strongly correlated with Cl^- in these maritime catchments), but there are exceptions to this rule (e.g., Br^-). Solutes that are weakly sorbing may most clearly express the spectral effects of dispersive mixing in the subsurface (*SI Appendix*). By contrast, there is a tendency toward shallower spectral slopes for some trace elements (e.g., Be, Se, Br^-, Mo, Cd, and Pb), which could arise because some of these elements are likely to be strongly sorbed to particulates (again, Se and Br^- are exceptions) and thus may undergo more episodic transport. Regardless of these individual differences, the most striking feature of the solute spectra is their overall consistency with $1/f$ scaling.

For chemically passive solutes derived primarily from atmospheric deposition, including ^{18}O, ^{2}H, and (in maritime settings) Cl^-, these catchments act as fractal filters, converting nearly white-noise atmospheric inputs into fractal $1/f$ streamflow outputs (10, 21, 22). The spectral slopes of Cl^-, a chemically passive tracer of sea salt deposition, are 0.41 ± 0.02 in precipitation and 1.29 ± 0.05 and 1.40 ± 0.06 in Upper and Lower Hafren streamflow, respectively (means ± SEs), implying that these catchments act as spectral filters with a $1/f$ fractal signature (i.e., the ratio between the output and input spectra scales as $1/f$). Fractal filtering of atmospheric inputs has been previously observed for Cl^-, not only at Plynlimon (10) but also in other geologically diverse catchments (21, 23, 24), suggesting that our observations may be broadly applicable.

Origins of Fractal Scaling. The $1/f$ scaling that we observe is not restricted to atmospherically sourced, chemically passive solutes like Cl^-, but instead is universal across a wide range of solutes, with widely varying chemical characteristics and diverse sources in the natural environment. For example, mass balance calculations show that Li, Be, Mn, Fe, Co, and U are predominantly (>90%) derived from sources within the Upper Hafren catchment rather than from atmospheric deposition (*SI Appendix*, Table S3). Nonetheless, these analytes all have spectral slopes of 0.88–1.09, similar to the $1/f$ signature of atmospherically sourced tracers. Likewise, the toxic metals Be, Cr, Co, Ni, Cu, Zn, As, Se, and Pb have widely varying degrees of chemical reactivity, but they all have spectral slopes of 0.85–1.21 in Upper Hafren streamwater. And the universal spectral signature is not attributable to strong correlations between the time series of the various solutes, because the average r^2 between pairs of solutes is less than 0.1.

Thus, the mechanisms behind the observed $1/f$ scaling cannot depend on the particular chemical characteristics of the solutes themselves. One-over-*f* noise was first observed almost a century ago in electrical circuits (25), and later in a wide variety of natural phenomena (26, 27), with many diverse theoretical models being proposed to explain it (28). Many proposed explanations involve superpositions of random fluctuations that relax or diffuse over a wide range of time scales (29). Analogous mechanisms operate in catchments, where chemical signals originate from many different points on the landscape and undergo widely varying degrees of dispersion as they are transported to the stream. Under these general conditions, as we show in the *SI Appendix*, random chemical fluctuations across the landscape—arising from atmospheric deposition or biogeochemical processes, for example—can be transformed into $1/f$ fluctuations in stream chemistry by both Fickian and so-called "anomalous" dispersion. Other models have also been proposed, including continuous-time random walks (30) and simulations combining advective–dispersive groundwater transport with spatially explicit subsurface heterogeneity (31), with in-channel mixing (32), and with vadose-zone and land-surface processes (33). (One-over-*f* noises are also often attributed to self-organized criticality, but this is not a plausible explanation here because the physical mechanisms controlling solute concentrations in natural waters do not resemble critical phase transitions.) In addition to the hillslope-scale advection–dispersion processes outlined in the *SI Appendix*, in larger river basins the branching structure of the river network could introduce additional geomorphological dispersion of chemical fluctuations (34). However, because travel through the channel network is much faster than hillslope transport, hillslope processes should normally dominate the transport response observed at the basin scale (35).

In contrast to the solute concentrations, stream discharge itself is distinctly nonfractal, scaling as white noise (slope of zero) at low frequencies and approximately as a random walk (slope of 2)

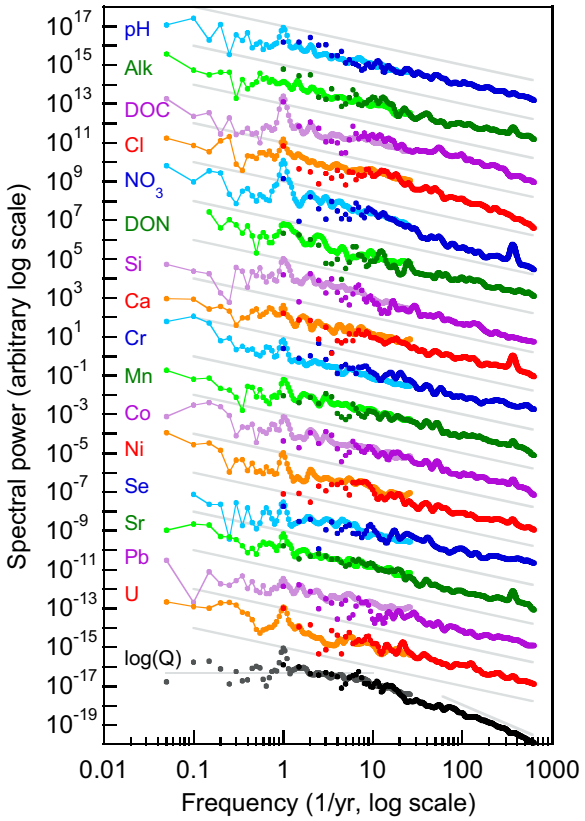

Fig. 2. Power spectra for concentration time series of 16 selected solutes in Upper Hafren streamwater at Plynlimon, Wales, from 22 mo of sampling at 7-h intervals (darker symbols) and up to 21 y of weekly sampling (lighter symbols). Power spectra from weekly and 7-h sampling of the logarithm of stream discharge are shown in gray and black for comparison. The slopes of all concentration spectra are close to $1/f$ scaling, shown by gray lines. In contrast, stream discharge exhibits white noise scaling for frequencies below ~5 per year, steepening to ~$1/f^2$ at frequencies of ~80–600 per year (short gray lines show slopes of zero and 2 for comparison). Spectra for individual solutes have been shifted by arbitrary factors to allow them to be visualized together. Spectra for all 45 solutes and both sites are shown in *SI Appendix*, Fig. S6.

at high frequencies (Fig. 2). This spectral behavior can be readily explained by the steep nonlinear dependence of discharge on catchment water storage (36), which prevents catchment storage from either filling too far (because any excess will run off) or draining too much (because discharge will rapidly decline). Thus, on time scales much longer than individual storm recessions, average stream discharge must approximately equal average atmospheric forcing by precipitation and evapotranspiration. On monthly and longer time scales, this forcing resembles white noise at Plynlimon, and thus discharge does as well. On much shorter time scales, catchment storage integrates fluctuations in atmospheric forcing over time. This integro-differential relationship (36) implies that storage fluctuations (and thus discharge fluctuations, which are functionally linked to them) should have a spectral slope equaling that of the atmospheric forcing, plus 2, at these shorter time scales—hence the spectral slope near 2 at high frequencies.

Implications for Water Quality Trend Detection. The universal $1/f$ scaling of solute concentrations, as shown in Figs. 2 and 3 and *SI Appendix*, Fig. S6, poses significant challenges to detecting changes and quantifying trends in water quality. This $1/f$ scaling implies that these time series contain equal spectral power (and thus equal variance) in each octave of frequency; this has the important consequence that averages taken over longer and longer intervals of time do not converge toward a stable value (27, 37), in contrast to white noise processes, for which the central limit theorem guarantees convergence at the familiar rate of $n^{-0.5}$. Despite its longstanding importance as a limit to measurement precision (27, 37), this non–self-averaging behavior has often remained unrecognized in environmental analysis.

Fig. 4 and *SI Appendix*, Fig. S10 illustrate the issue. Here we plot the rms differences between adjacent pairs of local averages, as a function of the length of time over which those averages are calculated. The leftmost points show the rms differences between successive individual 7-h samples; the next points show the rms differences between successive means of two 7-h samples, and so forth. The rightmost points show the rms deviations between successive 5- or 10-y averages (depending on the length of the available record), each composed of roughly 250 or 500 weekly samples. As the figures show, these long-term averages are typically about as variable, one from the next, as individual weekly or 7-h samples.

The non–self-averaging behavior described by the horizontal rms traces in Fig. 4 and *SI Appendix*, Fig. S10 contrasts sharply with the convergence of means predicted by the central limit theorem (shown by the slope of the heavy gray lines). The observed non–self-averaging behavior goes beyond just long-term persistence, as exemplified by the well-known Hurst effect (38), which often describes stationary processes in which means converge, but do so more slowly than $n^{-0.5}$ (weak self-averaging). However, the rms traces also show little evidence of nonstationary drift or secular trends, which would cause the rms values to increase with increasing time scale. Instead, the rms traces, along with the $1/f$ power spectra, suggest that these solute time series are poised at the threshold separating stationarity from nonstationarity.

In contrast to the solute concentrations, both stream discharge and its logarithmic transform (shown in black and dark gray in Fig. 4) exhibit conventional self-averaging behavior (shown by

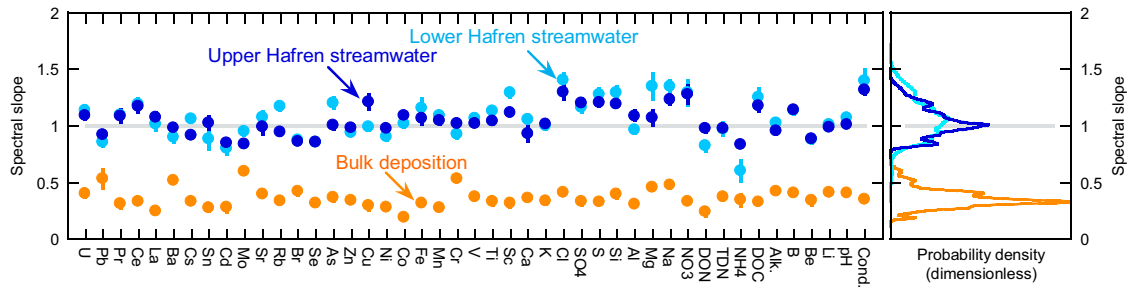

Fig. 3. Spectral slopes of all 45 water quality time series in Upper and Lower Hafren streamwater (dark blue and light blue symbols, respectively) and bulk precipitation at Plynlimon, Wales. Error bars show SEs, where these are larger than the plotting symbols. Gray line indicates spectral slope of 1 ($1/f$ noise).

the slope of the heavy gray lines) at time scales longer than ~1 mo, with averages becoming steadily less variable over longer averaging time scales. The time scales over which discharge is self-averaging correspond approximately to the frequency range where the discharge spectrum exhibits white-noise scaling (Fig. 2). The solute concentrations, by contrast, show no general tendency toward white-noise scaling at low frequencies or toward self-averaging behavior at long time scales.

The non–self-averaging behavior of the solute concentrations implies that their long-term variability is much greater than one would expect from their short-term behavior. One practical consequence of this phenomenon is that statistically significant trends in water quality can arise much more frequently, on all time scales, than one might expect. These trends are also poor predictors of future trends. For example, among the 45 solutes and the two streamflow sampling sites, there are a total of 1,655 individual solute-years for which annual trends can be fitted from the weekly sampling data, and 18% of these trends—180× the number expected to arise by chance—are statistically significant

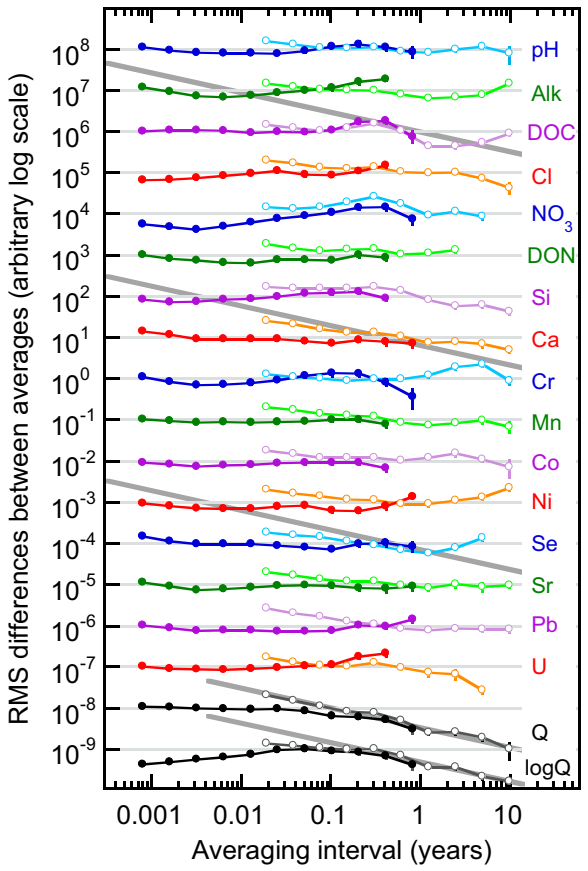

Fig. 4. Non–self-averaging behavior in water quality time series, illustrated by rms differences between successive mean concentrations of selected solutes in 7-h and weekly samples of Upper Hafren streamwater (solid and open symbols, respectively) averaged over intervals ranging from 7 h to 5–10 y. Error bars show SEs. Thin gray reference lines show trends for non–self-averaging behavior, in which averages over longer and longer time scales do not converge. Heavy gray lines show the slope of −0.5 predicted by the central limit theorem for self-averaging time series. The solutes generally plot as horizontal lines, indicating non–self-averaging behavior. In contrast, stream discharge and its logarithmic transform both follow the self-averaging behavior indicated by the heavy gray lines, for time scales longer than ~0.1 y. Individual solutes are shifted by arbitrary factors so they can be plotted together. Plots for all 45 solutes and both sampling sites are shown in *SI Appendix*, Fig. S10.

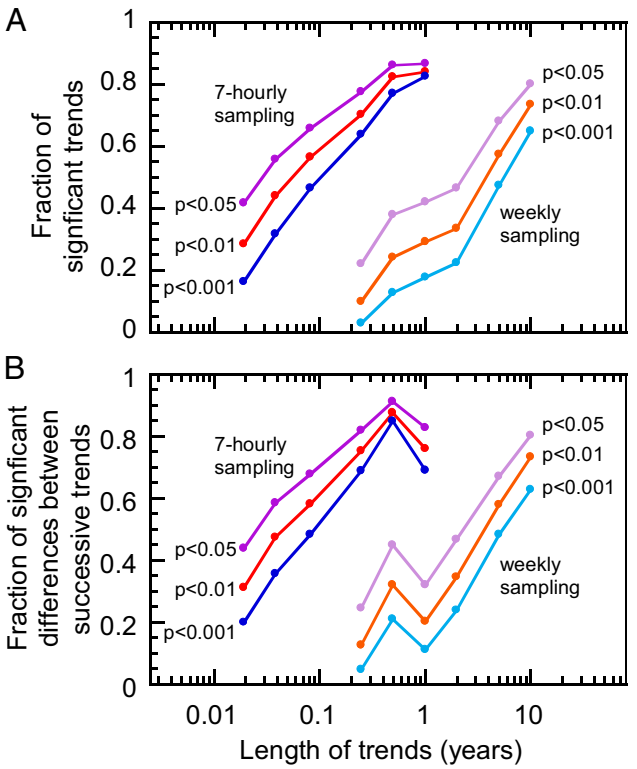

Fig. 5. Statistically significant but unreliable trends in water quality time series. (*A*) Prevalence of statistically significant trends: proportion of linear regression trends, calculated over intervals ranging from 7 d to 10 y, that are significantly different from zero ($P < 0.05$, $P < 0.01$, and $P < 0.001$, by two-tailed t test) in weekly and 7-h water quality time series. Reported proportions are averaged across all 45 solutes at both stream sampling sites. (*B*) Prevalence of unreliable trends: proportion of trends, calculated over intervals ranging from 7 d to 10 y, that are different from the immediately preceding trend of the same length (at the stated statistical significance level, by two-tailed t test). Reported proportions are averaged across all 45 solutes at both stream sampling sites. The peak at approximately the half-year mark arises from the seasonal cycles observed in many solutes.

at $P < 0.001$ when assessed by conventional t tests (Fig. 5*A*). However, these same trends are unreliable guides to future trends; for example, 11% of the annual trends in the weekly data are statistically different ($P < 0.001$) from the immediately preceding annual trends of the same solutes.

Surprisingly, having more data makes these problems much worse. The counterintuitive behavior outlined above becomes more pronounced, not less, with longer time series and more intensive sampling. As Fig. 5 shows, 65% of all of the 10-y linear regression trends in streamwater are statistically significant at $P < 0.001$ by conventional t tests, and over 60% of such 10-y trends are significantly different ($P < 0.001$) from the immediately preceding 10-y trends in the same solutes, indicating that even such long-term trends are unreliable predictors of future trends. Even higher proportions of statistically significant trends, and higher proportions of statistically significant differences between successive trends, are found in the 7-h water quality time series than in the weekly data (Fig. 5).

These examples show that water quality can be surprisingly dynamic and unpredictable across a wide range of solutes and time scales. This behavior defies naive expectations that water quality should have stable means and smooth trends, and confounds conventional statistical approaches that assume a clear separation of time scales between the signal and the surrounding noise. Such approaches will overestimate the significance, and

underestimate the uncertainty, of trends in multiscale time series (39). Alternative statistical methods are available for handling such time series (40–43), but outside of climate trend detection (42, 44), they have rarely been applied in environmental analysis.

The prevalence of coherent but continually shifting trends is characteristic of the non–self-averaging behavior of these 1/*f* time series. In contrast to classical examples of 1/*f* "noise" (37), however, the non–self-averaging in these natural systems does not primarily arise from measurement uncertainties per se. Thus, the 1/*f* noise in water quality is not strictly noise, but rather a signal reflecting natural processes; it arises primarily because catchments store, transport, and dispersively mix solutes over a wide range of space and time scales, as described in the *SI Appendix*.

In addition to these storage, transport, and mixing processes, water quality dynamics will also reflect the time series behavior of chemical inputs and within-catchment chemical reactions. Unambiguously distinguishing these different influences on water quality time series can be problematic. This problem highlights the need for better estimates of the time scales over which catchments store and mix solutes. These time scales can be used to set an approximate upper bound on the length of trends that could plausibly be artifacts of solute storage and mixing, and conversely to set a lower bound on the length of trends that could be unambiguously attributed to external forcing or biogeochemical processes.

Two aspects of catchment storage complicate efforts to quantify storage time scales, however. First, catchment storage includes both a dynamic component, which fills and drains in response to precipitation, and a residual component that remains even under dry conditions. Although dynamic storage can be inferred from streamflow variations (36), residual storage often accounts for most of a catchment's total storage and chemical "memory" (36, 45). The relatively large volume of residual storage, in comparison with the relatively small range of dynamic storage variations, implies that catchments' chemical memory can be much longer than their timescales of hydrologic response to rainfall. Residual storage cannot be estimated from catchment hydrologic behavior, but rather must be inferred from the behavior of passive tracers such as Cl^-, ^2H, and ^{18}O (10, 21, 45).

Second, to the extent that this residual storage is bypassed by high flows (rather than flushed out by them), a catchment's chemical memory can be much longer and more variable than one would infer from its steady-state mean residence time, as estimated by dividing the storage volume by the mean flow rate. The fractal 1/*f* spectra observed in passive tracers in many diverse catchments (21) imply that catchment storage is not characterized by conventional "mixing-tank" dynamics with a fixed characteristic timescale, for which the expected spectral scaling would be $1/f^2$ (10, 46). Although catchments are often modeled as well-mixed reservoirs, such conceptual models are not congruent with physical reality: a catchment simply has no compartment where its entire subsurface storage is continually and completely mixed, and there is no physical mechanism by which such mixing could occur. Instead, the observed 1/*f* spectra are much more consistent with dispersive mixing processes, operating in heterogeneous subsurface media and exhibiting a broad spectrum of residence time scales (21, 46, 47), which may also vary with changes in the temporal patterns of rainfall and evapotranspiration (48–50).

The universal 1/*f* spectrum of stream chemistry implies that catchment storage, transport, and mixing can generate visually and statistically convincing trends in surface water quality across a wide range of solutes and time scales. These trends may be hard to distinguish from other water quality trends that arise from long-term changes in nutrient or pollutant inputs, for example, or from biogeochemical reactions. Inferring changes in catchment inputs or biogeochemical process rates from temporal patterns in stream water quality must therefore be approached with caution.

Materials and Methods

Sampling and Chemical Analysis. Our chemical time series come from two small catchments, Upper Hafren and Lower Hafren (1.22 and 3.58 km^2, respectively) at Plynlimon, Wales (*SI Appendix*, Fig. S1). The Upper Hafren is predominantly moorland, whereas the Lower Hafren is predominantly Sitka spruce plantation. Bulk deposition was sampled using continuously open collectors in a moorland clearing at Carreg Wen at the edge of the Upper and Lower Hafren catchments. Bulk deposition and streamflow were sampled manually once each week, beginning in 1983 at Lower Hafren and 1990 at Upper Hafren (19). During a 2-y intensive sampling campaign (2007–2009), this manual sampling was supplemented by autosamplers that collected 24 samples per week, one sample every 7 h (17). On return to the laboratory, the samples were filtered (0.45 μm) followed by analysis using standard methods, including inductively coupled plasma (ICP) optical emissions spectroscopy (for major cations, B, total S, and Si), ICP-MS (for trace elements), and ion chromatography (for anions). Sampling sites and methods are described in more detail in the *SI Appendix*, and the raw data and metadata are provided in Datasets S1 and S2.

Conditioning of Time Series. We transformed several time series that exhibited strong nonstationarity in variance or strongly skewed distributions. We also normalized each time series for correlations with stream discharge to minimize the confounding influence of streamflow variations (51, 52). At Plynlimon, acidic soils overlie more alkaline bedrock (53), resulting in strong correlations between several analytes and the logarithm of stream discharge. For five solutes in particular (pH, alkalinity, Ca, Al, and Si), the underlying chemical fluctuations are obscured by streamflow variations, with the result that the 1/*f* spectral signature of the chemical dynamics is strongly overprinted by the spectrum of log(Q) (*SI Appendix*, Fig. S4). Likewise, for these five solutes, the non–self-averaging behavior of the chemical dynamics is overprinted, at time scales of months and longer, by the self-averaging behavior of log(Q). Correcting the chemical time series for flow-dependent variations by taking residuals of smooth splines fitted to the concentration–discharge relationship (*SI Appendix*, Fig. S3 and Table S4) reveals the underlying 1/*f* spectral signature and the corresponding non–self-averaging behavior for these five solutes. That is, the power spectra (Fig. 2) and rms traces (Fig. 4) of these five solutes closely resemble those of the other 40 solutes when the time series are flow-corrected, but would more closely resemble those of log(Q) if the time series were not flow-corrected. For the other 40 solutes, flow-correcting the chemical time series does not substantially affect the power spectra or the rms traces. Nonetheless, for the sake of consistency, all 45 chemical time series were flow-corrected before analysis (see *SI Appendix* for details).

Estimation of Power Spectra. Data gaps occurred intermittently due to autosampler failure or analytical problems, and also whenever rainfall yielded insufficient volume for chemical analysis. Such gapped time series require special Fourier analysis techniques, particularly for reddened spectra such as $1/f^{\alpha}$ noises, because spectral leakage from low frequencies with high power can contaminate the higher frequencies in the spectrum where the true signal is weaker. We used an adaptation of Foster's weighted wavelet transform (54) to suppress this leakage in estimating the spectrum. Because the gapped sampling has a regular (weekly or 7-h) time base, we used Kirchner's filtering method (55) to correct for spectral aliasing, which would otherwise lead to artificial flattening of the spectrum at high frequencies. In the *SI Appendix* we describe the computational details of our spectral methods and present the results of benchmark tests. All of our source codes (written in C) are available from the corresponding author.

ACKNOWLEDGMENTS. The Centre for Ecology and Hydrology (CEH) has supported the Plynlimon hydrochemical monitoring study for nearly three decades. For their long-term contributions to this effort, we thank the Plynlimon field staff at CEH Bangor, led by Brian Reynolds, and the analytical laboratory staffs at CEH Wallingford and CEH Lancaster, led by Margaret Neal and Phil Rowland, respectively. During early phases of this work, J.W.K. received support from the Berkeley Water Center and the Miller Institute for Basic Research.

1. Smith RA, Alexander RB, Wolman MG (1987) Water-quality trends in the nation's rivers. *Science* 235(4796):1607–1615.
2. Stoddard JL, et al. (1999) Regional trends in aquatic recovery from acidification in North America and Europe. *Nature* 401(6753):575–578.
3. Monteith DT, et al. (2007) Dissolved organic carbon trends resulting from changes in atmospheric deposition chemistry. *Nature* 450(7169):537–540.
4. Handy RD (1994) Intermittent exposure to aquatic pollutants: Assessment, toxicity and sublethal responses in fish and invertebrates. *Comp Biochem Physiol C Pharmacol Toxicol Endocrinol* 107(2):171–184.
5. Reinert KH, Giddings JM, Judd L (2002) Effects analysis of time-varying or repeated exposures in aquatic ecological risk assessment of agrochemicals. *Environ Toxicol Chem* 21(9):1977–1992.
6. Gordon AK, Mantel SK, Muller NWJ (2012) Review of toxicological effects caused by episodic stressor exposure. *Environ Toxicol Chem* 31(5):1169–1174.
7. Lepori F, Keck F (2012) Effects of atmospheric nitrogen deposition on remote freshwater ecosystems. *Ambio* 41(3):235–246.
8. Peterson BJ, et al. (2001) Control of nitrogen export from watersheds by headwater streams. *Science* 292(5514):86–90.
9. Alexander RB, Boyer EW, Smith RA, Schwarz GE, Moore RB (2007) The role of headwater streams in downstream water quality. *J Am Water Resour Assoc* 43(1):41–59.
10. Kirchner JW, Feng X, Neal C (2000) Fractal stream chemistry and its implications for contaminant transport in catchments. *Nature* 403(6769):524–527.
11. McGuire KJ, McDonnell JJ (2006) A review and evaluation of catchment transit time modeling. *J Hydrol (Amst)* 330(3-4):543–563.
12. Burns DA, et al. (2001) Quantifying contributions to storm runoff through end-member mixing analysis and hydrologic measurements at the Panola Mountain Research Watershed (Georgia, USA). *Hydrol Processes* 15(10):1903–1924.
13. Boyer EW, Hornberger GM, Bencala KE, McKnight DM (1997) Response characteristics of DOC flushing in an alpine catchment. *Hydrol Processes* 11(12):1635–1647.
14. Bowes MJ, Smith JT, Neal C (2009) The value of high-resolution nutrient monitoring: A case study of the River Frome, Dorset, UK. *J Hydrol (Amst)* 378(1-2):82–96.
15. Cassidy R, Jordan P (2011) Limitations of instantaneous water quality sampling in surface-water catchments: Comparison with near-continuous phosphorus time-series data. *J Hydrol (Amst)* 405(1-2):182–193.
16. Pellerin BA, et al. (2012) Taking the pulse of snowmelt: In situ sensors reveal seasonal, event and diurnal patterns of nitrate and dissolved organic matter variability in an upland forest stream. *Biogeochemistry* 108(1-3):183–198.
17. Neal C, et al. (2012) High-frequency water quality time series in precipitation and streamflow: From fragmentary signals to scientific challenge. *Sci Total Environ* 434: 3–12.
18. Neal C, et al. (2013) High-frequency precipitation and stream water quality time series from Plynlimon, Wales: An openly accessible data resource spanning the periodic table. *Hydrol Processes*, 10.1002/hyp.9814.
19. Neal C, et al. (2011) Three decades of water quality measurements from the Upper Severn experimental catchments at Plynlimon, Wales: An openly accessible data resource for research, modelling, environmental management and education. *Hydrol Processes* 25(24):3818–3830.
20. Witt A, Malamud BD (2013) Quantification of long-range persistence in geophysical time series: Conventional and benchmark-based improvement techniques. *Surv Geophys*, in press.
21. Godsey SE, et al. (2010) Generality of fractal 1/f scaling in catchment tracer time series, and its implications for catchment travel time distributions. *Hydrol Processes* 24(12): 1660–1671.
22. Kirchner JW, Tetzlaff D, Soulsby C (2010) Comparing chloride and water isotopes as hydrological tracers in two Scottish catchments. *Hydrol Processes* 24(12):1631–1645.
23. Shaw SB, Harpold AA, Taylor JC, Walter MT (2008) Investigating a high resolution, stream chloride time series from the Biscuit Brook catchment, Catskills, NY. *J Hydrol (Amst)* 348(3-4):245–256.
24. Koirala SR, Gentry RW, Perfect E, Mulholland PJ, Schwartz JS (2011) Hurst analysis of hydrologic and water quality time series. *J Hydrol Eng* 16(9):717–724.
25. Johnson JB (1925) The Schottky effect in low frequency circuits. *Phys Rev* 26(1):71–85.
26. Mandelbrot BB, Wallis JR (1969) Some long-run properties of geophysical records. *Water Resour Res* 5(2):321–340.
27. Press WH (1978) Flicker noises in astronomy and elsewhere. *Comments Astrophys* 7(4): 103–119.
28. Weissman MB (1988) 1/f noise and other slow, nonexponential kinetics in condensed matter. *Rev Mod Phys* 60(2):537–571.
29. Dutta P, Horn PM (1981) Low-frequency fluctuations in solids: 1/f noise. *Rev Mod Phys* 53(3):497–516.
30. Scher H, Margolin G, Metzler R, Klafter J, Berkowitz B (2002) The dynamical foundation of fractal stream chemistry: The origin of extremely long retention times. arXiv:cond-mat/0202326.
31. Fiori A, Russo D (2008) Travel time distribution in a hillslope: Insight from numerical simulations. *Water Resour Res* 44(12):W12426, 10.1029/2008WR007135.
32. Lindgren GA, Destouni G, Miller AV (2004) Solute transport through the integrated groundwater-stream system of a catchment. *Water Resour Res* 40(3):W03511, 10.1029/2003WR002765.
33. Kollet SJ, Maxwell RM (2008) Demonstrating fractal scaling of baseflow residence time distributions using a fully-coupled groundwater and land surface model. *Geophys Res Lett* 35(7):L07402, 10.1029/2008GL033215.
34. Rinaldo A, Marani A, Rigon R (1991) Geomorphological dispersion. *Water Resour Res* 27(4):513–525.
35. Botter G, Rinaldo A (2003) Scale effect on geomorphological and kinematic dispersion. *Water Resour Res* 39(10):1286, 10.1029/2003WR002154.
36. Kirchner JW (2009) Catchments as simple dynamical systems: catchment characterization, rainfall-runoff modeling, and doing hydrology backward. *Water Resour Res* 45:W02429 10.01029/02008WR006912.
37. Halford D (1968) A general mechanical model for $|f|^{\alpha}$ spectral density random noise with special reference to flicker noise 1/|f|. *Proc IEEE* 56(3):251–258.
38. Hurst HE (1951) Long-term storage capacity of reservoirs. *Trans Am Soc Civ Eng* 116: 770–799.
39. Cohn TA, Lins HF (2005) Nature's style: Naturally trendy. *Geophys Res Lett* 32:L32402.
40. Beran J (1994) *Statistics for Long-Memory Processes* (Chapman & Hall/CRC, New York).
41. Fadili MJ, Bullmore ET (2002) Wavelet-generalized least squares: A new BLU estimator of linear regression models with 1/f errors. *Neuroimage* 15(1):217–232.
42. Bloomfield P, Nychka D (1992) Climate spectra and detecting climate change. *Clim Change* 21(3):275–287.
43. Koutsoyiannis D (2003) Climate change, the Hurst phenomenon, and hydrological statistics. *Hydrol Sci J* 48(1):3–24.
44. Mann ME (2011) On long range dependence in global surface temperature series. *Clim Change* 107(3-4):267–276.
45. Birkel C, Soulsby C, Tetzlaff D (2011) Modelling catchment-scale water storage dynamics: Reconciling dynamic storage with tracer-inferred passive storage. *Hydrol Processes* 25(25):3924–3936.
46. Kirchner JW, Feng X, Neal C (2001) Catchment-scale advection and dispersion as a mechanism for fractal scaling in stream tracer concentrations. *J Hydrol (Amst)* 254(1-4):81–100.
47. Feng XH, Kirchner JW, Neal C (2004) Measuring catchment-scale chemical retardation using spectral analysis of reactive and passive chemical tracer time series. *J Hydrol (Amst)* 292(1-4):296–307.
48. Hrachowitz M, Soulsby C, Tetzlaff D, Malcolm IA, Schoups G (2010) Gamma distribution models for transit time estimation in catchments: Physical interpretation of parameters and implications for time-variant transit time assessment. *Water Resour Res* 46(10):W10536, 10.1029/2010WR009148.
49. Birkel C, Soulsby C, Tetzlaff D, Dunn S, Spezia L (2012) High-frequency storm event isotope sampling reveals time-variant transit time distributions and influence of diurnal cycles. *Hydrol Processes* 26(2):308–316.
50. Botter G (2012) Catchment mixing processes and travel time distributions. *Water Resour Res* 48(5):W05545, 10.1029/2011WR011160.
51. Kirchner JW, Dillon PJ, LaZerte BD (1993) Separating hydrological and geochemical influences on runoff chemistry in spatially heterogeneous catchments. *Water Resour Res* 29(12):3903–3916.
52. Kirchner JW, Hooper RP, Kendall C, Neal C, Leavesley G (1996) Testing and validating environmental models. *Sci Total Environ* 183(1-2):33–47.
53. Neal C, Robson AJ, Smith CJ (1990) Acid neutralization capacity variations for the Hafren forest streams, mid-Wales: Inferences for hydrological processes. *J Hydrol (Amst)* 121(1-4):85–101.
54. Foster G (1996) Wavelets for period analysis of unevenly sampled time series. *Astron J* 112(4):1709–1729.
55. Kirchner JW (2005) Aliasing in $1/f^{(\alpha)}$ noise spectra: Origins, consequences, and remedies. *Phys Rev E Stat Nonlin Soft Matter Phys* 71(6 Pt 2):066110.